Electronic Supplementary Material (ESI) for Journal of Materials Chemistry C.

Supporting Information

Copper particle-free ink with enhanced performance for inkjet-printed flexible UWB antennas

Wendong Yang[a, b]*, Zhichao Dong[a, b], Zihao Guo[a, b] and Haoqiang Sun[a, b]

a. School of Electronic and Information Engineering, Liaoning Technical University, Huludao City, 125105, China.
*Email: wendong_2007@163.com; *corresponding author*
b. Key Laboratory of Radio Frequency and Big Data for Intelligent Applications, Liaoning Technical University, Huludao City, 125105, China.

Section 1 Antenna Design Processes

The proposed flexible UWB antenna is designed based on a monopole antenna. The following are the specific design steps of the antenna.

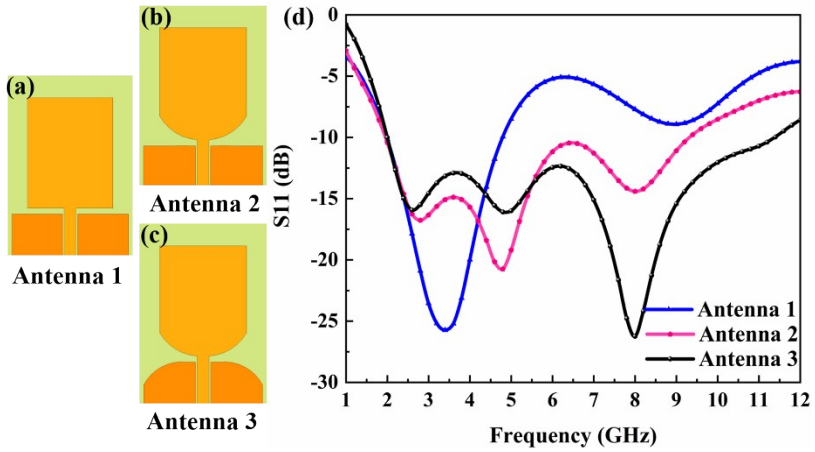

Figure S1. Design processes of the proposed flexible UWB antenna: (a-c) structures of Antenna 1-3, and (d) their return loss values

Step 1: Design of a conventional monopole antenna, named as Antenna 1.

In this step, a conventional monopole antenna with a minimum cutoff frequency of less than 3.1 GHz is designed using the cylinder approximation approach.[1] The antenna is fed by the coplanar waveguide approach and consists of a rectangular patch unit and a ground plate (Figure S1a). It has an operating bandwidth of 1.94-4.74GHz.

Step 2: Design of UWB antenna from Antenna1, named as Antenna 2.

Antenna 2 is built by doing fan-shaped gradient processing to the lower half of the radiation patch of Antenna 1 (Figure S1b), resulting in a larger bandwidth at 1.95-9.34GHz. However, the impedance matching of the Antenna 2 around 6GHz is not ideal.

Step 3: Structure optimization of Antenna 2, named as Antenna 3.

Antenna 3 is developed on the basis of Antenna 2 to further broaden the operating band for UWB, where the rectangular grounding plate of the antenna is cut into a circular arc shape and the gap size between the ground plate and the feeder is decreased (Figure 1c). As expected, the operating frequency band of the Antenna 3 is 2.0-11.39GHz, which covers the UWB band range.

Section 2 Optimization of Cuf ink

Inks with OA/DAP ratios ranging from 3:0 to 0:3 were formulated and named as Ink_1, Ink_2 Ink_3, Ink_4 and Ink_5, respectively. XRD, SEM and four-probe analyses were employed to investigate the physical phase, morphology and resistivity of the films from these inks to determine the optimal mixing

ratio; the results are given in **Figure. S2**.

Clearly, the XRD patterns of all the films exhibit a crystalline copper structure (JCPDS No. 04-0836, **Figure. S2a**), indicating that the copper-amine complex in each ink has been converted into metallic copper. **Figure. S2b** shows the resistivity data for each film. As the DAP content increases, the resistivity of the silver film decreases dramatically, however, there is an optimal ratio at which the resistance value is the lowest. **Figure S2c** shows the corresponding surface morphologies of each film on glass substrates. The surface morphology of the film from OA/DAP inks in 2:1 and 1:1 revealed a microstructure composed of copper particles with big and small sizes, where the latter was filled in the voids of the former. The film formed by the ink in 1:2 presented a microstructure consisting of larger copper nanoparticles in a good connection.

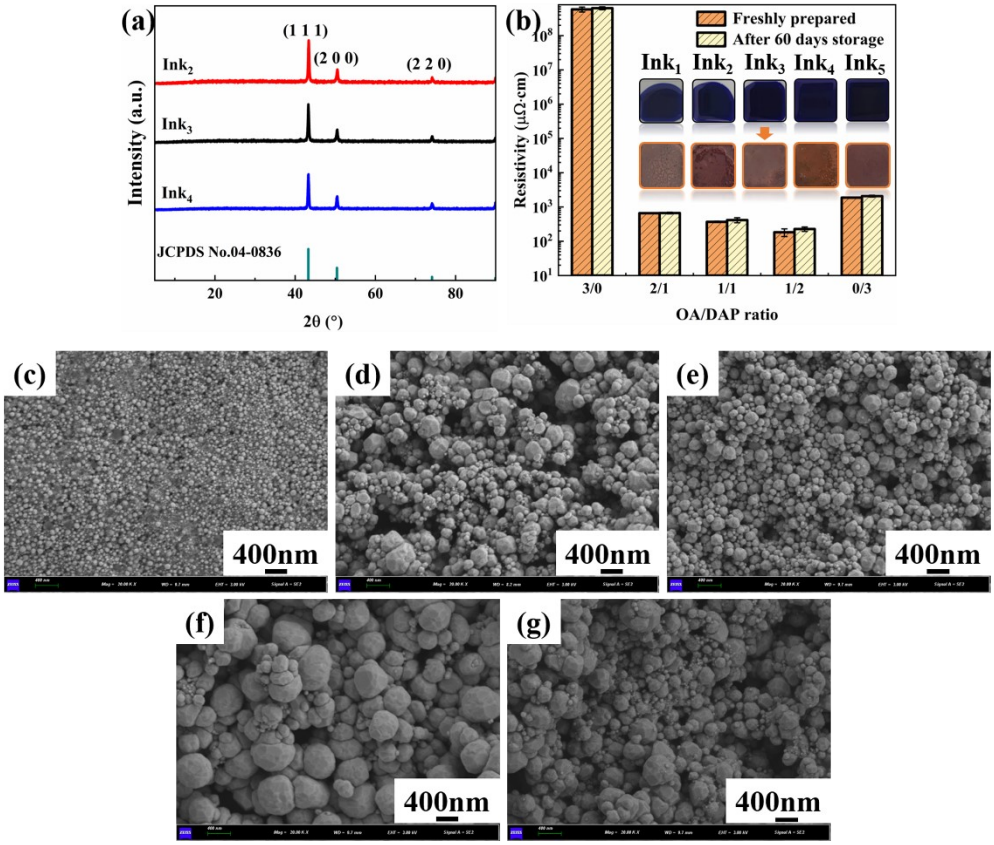

Figure S2. (a) XRD patterns, (b) resistivities and (c-g) surface morphologies of copper films produced at 170°C for 60 minutes from inks prepared with varied molar ratios of OA and DAP
(c) 3:0, (d) 2:1, (e) 1:1, (f) 1:2 and (g) 0:3

The particle size statistics of each copper film are shown in **Figure S3**. It can be found that with the increase of the DAP content, the average particle size of the obtained copper particles becomes larger, and these particles are well connected, thus the volume resistivity of the copper film decreases. The structure differences may be associated with the activating effect and capping effect of the OA and DAP.[2]

Here, considering the good electrical property and film morphology will be beneficial to the performance of the subsequent antenna, we chose 1:2 as the optimal ratio to formulate the ink for the later printing.

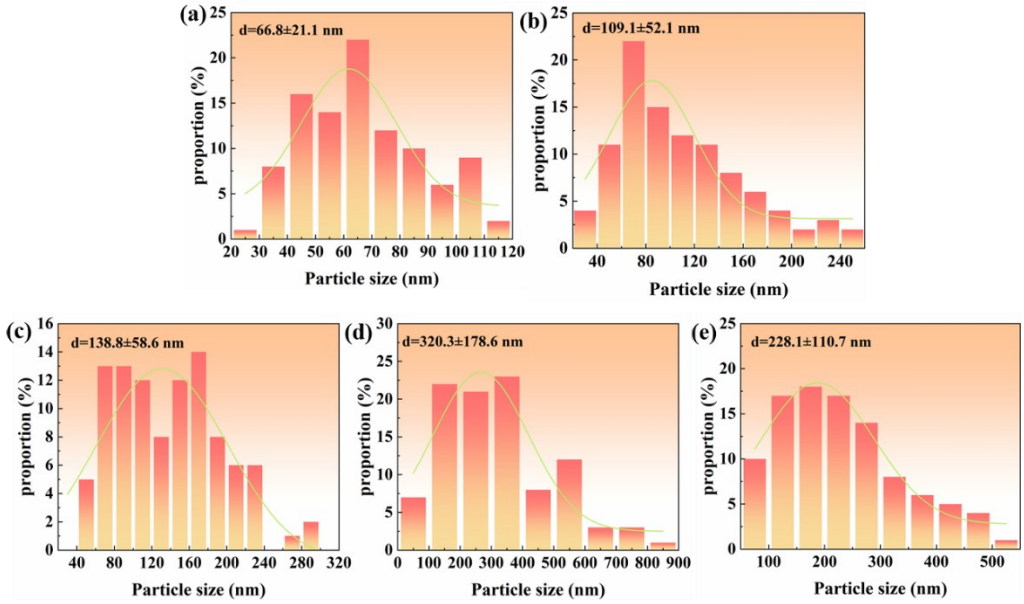

Figure S3. The corresponding particle size distributions of the copper films from Ink_1 to Ink_5

Section 3. Ink Stability

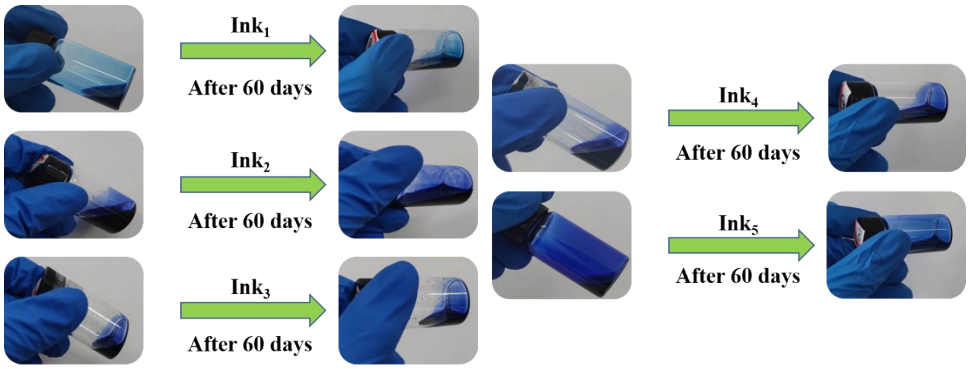

Figure S4. Photographs of Ink_1-Ink_5 freshly prepared and stored in a fridge at 5°C for 60 days

Section 4. Bendability of the printed antenna prototype

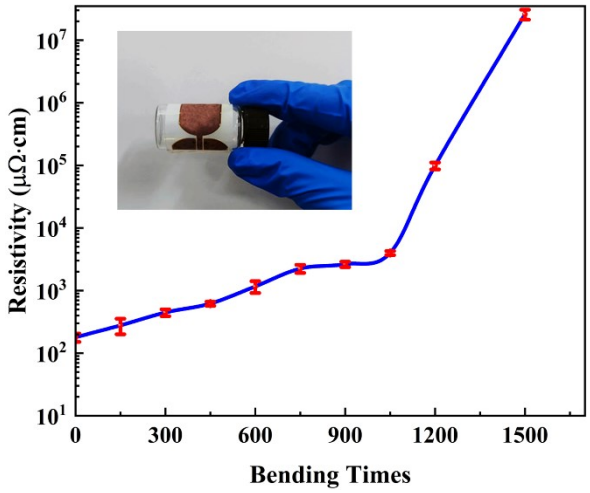

Figure S5. Bendability test of the antenna prototype

Section 4. Ink Comparison

Table S1 A brief overview of the reported copper-based particle-free inks

Reference	Ink Recipe			Patterning Method		Resistivity (μΩ·cm)	Advantages	Disadvantages
	Copper precursor	Complexing agent	Solvent	Deposition	Metallization			
[3]	Copper format	Hexylamine and 2-amino-2-methyl-1-propanol	Isopropyl alcohol	Spin coating	Laser sintering	17	Good conductivity, Tighter film structure	Not suitable for inkjet printing, 3 hours of ink preparation, and need a special sintering method
[4]	Copper (II) hydroxide	Formic acid and citric acid	DI water	Handwriting	Intensive Pulsed Light Sintering	3.21-5.27	Excellent conductivity	Not suitable for inkjet printing, and need a special sintering method
[5]	Copper (II) formate tetrahydrate	n-octyl amine	Toluene	Squeegee coating	140°C for 60min, N_2	20	Good conductivity, Lower sintering temperature,	Toxic ink solvent, not suitable for inkjet printing
[6]	Copper (II) formate anhydrate	3-dimethylamino-1,2-propanediol	/	Squeegee coating	180 °C for 5min	300	Air-sinterable	Conductivity, not suitable for inkjet printing
[7]	Copper (II) formate tetrahydrate	1,2-diaminopropane	Ethanol	Drop coating	180 °C, 1 min	18	Good conductivity, Air-sinterable,	Not suitable for inkjet printing
[8]	Copper (II) formate tetrahydrate	2-Amino-2-methyl-1-propanol	Isopropyl alcohol	Drop coating	350 °C for 30min, N_2	9.46	Excellent conductivity	Not suitable for inkjet printing, and high sintering temperature
[9]	Copper acetate	Cyclohexylamine	Ethanol/ethylene glycol mixture	Drop coating	230 °C for 60min, N_2	22	Good conductivity,	Not suitable for inkjet printing and high sintering temperature
[10]	Copper (II) formate hydrate	Hexylamine	/	Coating	250 °C for 2 min with formic acid	5.2	Excellent conductivity	Not suitable for inkjet printing, high sintering temperature with reductive atmosphere
[11]	Copper (II) formate tetrahydrate	2-amino-2-methyl-1-propanol	Diethylene glycol methyl ether and n-Butanol	Inkjet printing	190°C for 2 min, N_2	10.5	Good conductivity	/
[12]	Copper formate/acetate/oleate	Diethanolamine	Ethanol	Inkjet printing	Intensive Pulsed Light Sintering	56	Conductivity	Need a special sintering method
[13]	Copper(II) ethylene glycol carboxylates	/	DI water	Inkjet printing	300 °C, 10 min, N_2	66.7 (5 layers on PI)	Conductivity	High sintering temperature
This work	Copper (II) formate tetrahydrate	1,3-Diaminopropane and octylamine	Methanol	Inkjet printing	170°C for 60 min, N_2	127 (1 layer)	Excellent stability and printability Certain antioxidant property	Conductivity

References

1. R. Singh and G. Kumar, M. *Tech credit seminar report*, 2003, 1-24.
2. W. Xu and T. Wang, *Langmuir*, 2017, **33**, 82-90.
3. J. Lee, B. Lee, S. Jeong, Y. Kim and M. Lee, *Appl. Surf. Sci.*, 2014, **307**, 42-45.
4. B.-Y. Wang, T.-H. Yoo, Y.-W. Song, D.-S. Lim and Y.-J. Oh, *ACS Appl. Mater. Interfaces*, 2013, **5**, 4113-4119.
5. A. Yabuki, N. Arriffin and M. Yanase, *Thin Solid Films*, 2011, **519**, 6530-6533.
6. A. Yabuki, Y. Tachibana and I. W. Fathona, *Mater. Chem. Phys.*, 2014, **148**, 299-304.
7. Y. Dong, Z. Lin, X. Li, Q. Zhu, J.-G. Li and X. Sun, *J. Mater. Chem. C.*, 2018, **6**, 6406-6415.
8. D.-H. Shin, S. Woo, H. Yem, M. Cha, S. Cho, M. Kang, S. Jeong, Y. Kim, K. Kang and Y. Piao, *ACS Appl. Mater. Interfaces*, 2014, **6**, 3312-3319.
9. W.-d. Yang, C.-h. Wang, V. Arrighi, C.-y. Liu and D. Watson, *J. Mater. Sci.: Mater. Electron.*, 2015, **26**, 8973-8982.
10. S. J. Kim, J. Lee, Y.-H. Choi, D.-H. Yeon and Y. Byun, *Thin Solid Films*, 2012, **520**, 2731-2734.
11. Y. Farraj, M. Grouchko and S. Magdassi, *Chem. Commun.*, 2015, **51**, 1587-1590.
12. T. Araki, T. Sugahara, J. Jiu, S. Nagao, M. Nogi, H. Koga, H. Uchida, K. Shinozaki and K. Suganuma, *Langmuir*, 2013, **29**, 11192-11197.
13. D. Adner, F. M. Wolf, S. Möckel, J. Perelaer, U. S. Schubert and H. Lang, *Thin Solid Films*, 2014, **565**, 143-148.